Instanton Analysis of Hysteresis in the Three-Dimensional Random-Field Ising Model

Markus Müller and Alessandro Silva

Department of Physics, Rutgers University, Piscataway, New Jersey 08854, USA

(Received 20 June 2005; revised manuscript received 22 November 2005; published 21 March 2006)

We study the magnetic hysteresis in the random-field Ising model in 3D. We discuss the disorder dependence of the coercive field H_c, and obtain an analytical description of the smooth part of the hysteresis below and above H_c, by identifying the disorder configurations (instantons) that are the most probable to trigger local avalanches. We estimate the critical disorder strength at which the hysteresis curve becomes continuous. From an instanton analysis at zero field we obtain a description of local two-level systems in the ferromagnetic phase.

DOI: 10.1103/PhysRevLett.96.117202 PACS numbers: 75.10.Nr, 05.50.+q, 75.60.Ej

In disordered systems whose pure counterparts undergo a first order phase transition as an external parameter (e.g., field or pressure) is tuned, the presence of randomness leads to interesting hysteretic phenomena [1]. Those arise from local modifications of the spinodal point due to disorder, as well as from the presence of many metastable states. The simplest system exhibiting such phenomena is the random-field Ising model (RFIM), often studied as a representative model for hysteresis in the presence of random fields [2–7].

In the RFIM, the gradual transition between states of negative and positive magnetization proceeds via avalanches triggered by the increase of the external magnetic field. Previous studies [8,9] have shown that in the presence of strong disorder all avalanches are bounded and the hysteresis loop is macroscopically smooth. In weak disorder, however, there is a finite coercive field beyond which the ferromagnetic coupling induces macroscopic avalanches that span large parts of the sample and lead to a sharp jump in the hysteresis curve. The two disorder regimes are separated by a critical point which is believed to control the power law distribution of Barkhausen noise [10,11]. Recently, indications for such disorder induced transitions have been reported in disordered magnets [2,4] as well as in the context of capillary condensation in aerogels [7,12].

The hysteresis in the RFIM is intimately tied to the complexity of its free energy landscape, possessing an exponential number of metastable minima. However, the precise connection between the disorder induced energy landscape and the nature and extent of the avalanches has not been established. So far, studies of the hysteresis in the RFIM concentrated on lattice simulations at zero temperature [8,11], and most analytical insight was restricted to the Bethe lattice [9] or the extreme mean field limit [8] where all spins interact with each other. In this Letter, we make a first step towards an analytical theory for 3D systems. In particular, we analyze the features of the hysteresis loop as a function of disorder strength and sample size and characterize the typical avalanches occurring along the hysteresis loop. This provides a new perspective on the above-mentioned disorder induced transition. Further, by studying typical configurations that trigger avalanches at zero field we obtain insight into metastability in the ferromagnetic phase.

Before giving the details of our analysis, we summarize the qualitative picture we have obtained, concentrating on the raising branch of the saturation hysteresis loop (see Fig. 1). In a pure system, hysteresis arises due to the metastability of the negatively magnetized state in external

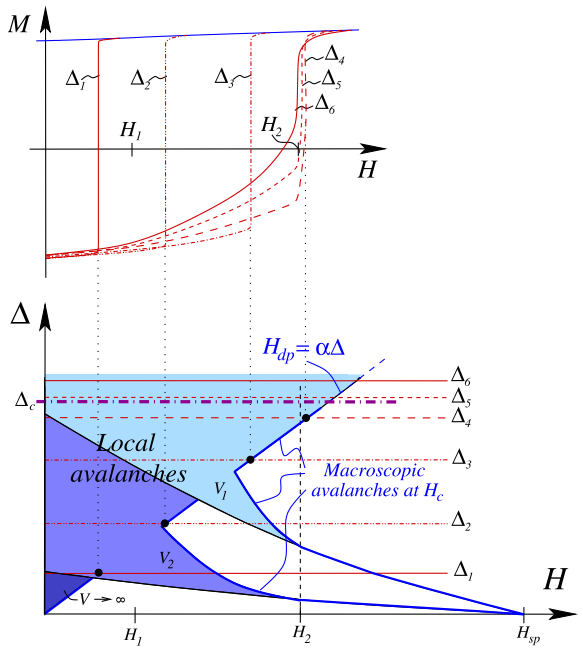

FIG. 1 (color online). Top: Hysteresis curves for increasing disorder. At the coercive field H_c the magnetization jumps discontinuously. In strong disorder ($\Delta > \Delta_c \approx \Delta_5$) the jump disappears since bubbles are already dense at H_{dp}. Bottom: The shaded areas indicate where local avalanches are observed in the $H - \Delta$ plane [in finite volumes $V_1 < V_2 < \infty$ (lighter shaded), and for $V = \infty$ (dark area, $H < H_{dp} = \alpha\Delta$)]. Macroscopic avalanches occur at the coercive field H_c (thick blue line). The horizontal lines correspond to the hysteresis curves in the top panel.

 © 2006 The American Physical Society

fields H below the spinodal field H_{sp}. This simple scenario is strongly modified by disorder: Because of rare regions with strong positive fields, bubbles of positive magnetization are created spontaneously at any small H. However, they are prevented from spreading by disorder induced pinning. The latter leads to a finite coercive field H_c which grows with disorder strength. For fields below H_c, the magnetization curve is determined by small avalanches, triggered by the increase of H. At H_c sample spanning avalanches occur, while beyond H_c only small regions with strong negative random fields may resist the invasion of the positively magnetized phase, finally collapsing under further increase of the field. With increasing disorder strength, the local avalanches become so dense that the emerging bubbles already percolate before the threshold for unlimited spread, H_c is reached. In this situation, there is no room for avalanches to spread at H_c, and the hysteresis loop becomes continuous.

In order to study the nature of avalanches in the 3D RFIM, we have analyzed its continuum version, described by the standard Landau-Ginzburg free energy

$$\bar{F} = F_0 \int d\mathbf{x} \left[\frac{1}{2}(\nabla\varphi)^2 + \bar{V}(\varphi) - \bar{H}\varphi - \bar{h}(\mathbf{x})\varphi \right]. \quad (1)$$

Here $\varphi(\mathbf{x})$ is the coarse-grained magnetization whose tendency towards ferromagnetism is described by the potential $\bar{V}(\varphi) = \frac{m^2}{2}(\varphi)^2 + \frac{g}{4}(\varphi)^4$ with the reduced temperature $m^2 \propto \tau \equiv -(1 - T/T_c)$. $\bar{H}$ is the uniform external magnetic field, and $\bar{h}(\mathbf{x})$ is a Gaussian random field with zero mean and variance $\langle \bar{h}(\mathbf{x})\bar{h}(\mathbf{x}')\rangle = \bar{\Delta}\,\delta(\mathbf{x} - \mathbf{x}')$. The prefactor F_0 depends on the microscopic details and increases with the range of ferromagnetic interactions.

We only consider $T < T_c$ ($m^2 < 0$) which is necessary to ensure the presence of metastable states. It is convenient to rescale all quantities according to natural units, $\mathbf{r} = \mathbf{x}/\ell$, $\Psi(\mathbf{r}) = \varphi(\mathbf{x})/\varphi_0$, $h(\mathbf{r}) = (\ell^2\bar{h}(\mathbf{x}))/(2\varphi_0)$, and $H = (\ell^2\bar{H})/(2\varphi_0)$, where $\varphi_0 = (|m^2|/g)^{1/2}$ is the equilibrium magnetization of the pure system and $\ell = (2/m^2)^{1/2} \sim \tau^{-1/2}$ is the mean field correlation length. The reduced disorder strength is $\Delta = (\bar{\Delta}\ell)/(4\varphi_0^2) \sim (\bar{\Delta})\tau^{-3/2}$. Further, we denote by $\Psi_{\pm}(H)$ the minimum with positive or negative magnetization of $V(\Psi) - H\Psi$, where $V(\Psi) = -\frac{1}{2}\Psi^2 + \frac{1}{4}\Psi^4$.

In order to study the free energy landscape of this model, we restrict ourselves to a mean field analysis and concentrate on local extrema of (1), satisfying

$$\frac{\delta F}{\delta\Psi(\mathbf{r})} = -\frac{1}{2}\nabla^2\Psi(\mathbf{r}) + V'(\Psi(\mathbf{r})) - H - h(\mathbf{r}) = 0. \quad (2)$$

In the spirit of the rate independent hysteresis approximation [13] we focus on spontaneously occurring events and neglect thermal activation. This is justified sufficiently far below T_c where typical free energy barriers between local minima are larger than T [14].

We may restrict the analysis of the hysteresis loop to the raising branch where the magnetization is everywhere close to $\Psi_-(H)$ at sufficiently negative H. As H is increased, the magnetization either remains in its local free energy minimum, responding paramagnetically to the field change, or it becomes locally unstable, and a bubble with higher magnetization is created spontaneously. This requires a sufficiently strong local excursion $h(\mathbf{r})$ of the random field. For weak disorder such configurations are rare, their density scaling as $\rho \propto \exp[-S]$, where $S = \int d\mathbf{r}[h(\mathbf{r})]^2/2\Delta$. Hence, we may think of them as dilute islands each of which can be analyzed separately. Further, we may assume that at some distance from a rare excursion, the random fields are weak such that the magnetization tends to Ψ_-.

The fate of a spontaneously emerging bubble depends on its size. We will see that typical bubbles are small and do not spread much since they are held back by a surface tension barrier. However, this does not apply to larger (and hence exponentially rarer) bubbles. Instead, their dynamics is governed by the competition between the external field exerting a driving force $2H$ on the surface of the bubble, and the random-field disorder, which tends to pin it. Collective pinning theory predicts the critical field for domain wall depinning to scale as $H_c = \alpha\Delta$ [15]. From a high velocity expansion [16] we obtained the estimate $\alpha \approx 0.055$, which we confirmed by numerical simulations [17]. For $H < H_c$, all avalanches are bounded, and the hysteresis loop is dominated by typical, i.e., most abundant, small avalanches. Beyond H_c, the *first* unstable bubble which is not constrained by surface tension induces a sample spanning avalanche and a macroscopic jump in magnetization, however low the probability per unit volume for such an event may be. In the thermodynamic limit, the coercive field H_c thus coincides with the depinning field H_{dp}. We will discuss mesoscopic fluctuations of H_c in weakly disordered small samples further below. The approach to complete saturation beyond H_c is governed by small bubbles of negative magnetization that spontaneously implode upon an increase of field.

Let us now analyze in more detail the properties of typical avalanches as a function of disorder and field, both for $H < H_c$ and $H > H_c$. An avalanche is triggered spontaneously when a local free energy minimum [with magnetization $\Psi(r)$] becomes unstable upon increase of H. This occurs when $\Psi(r)$ merges with an adjacent saddle point, $\Psi_{sp}(r)$, the magnetization difference $\delta\Psi = \Psi_{sp} - \Psi$ turning into a soft mode of the Hessian,

$$[-1/2\nabla^2 + V''(\Psi)]\delta\Psi = 0. \quad (3)$$

Let us denote by $\mathcal{M}$ the set of all states Ψ, such that there is a soft mode $\delta\Psi$ satisfying Eq. (3). These states are ''marginal'' in the sense that they are unstable with respect to the smallest perturbations.

Typical avalanches are triggered by the most probable configurations (''instantons'') of random fields, $h = h_{inst}(\mathbf{r}|H')$, such that the current magnetization state, $\Psi(\mathbf{r})$, becomes marginal ($\Psi \in \mathcal{M}$) when the external field reaches H'. These instantons thus correspond to nontrivial

local minima of the action

$$S=\frac{1}{2\Delta}\int d\mathbf{r}h^2(\mathbf{r})=\frac{1}{2\Delta}\int d\mathbf{r}\left[\frac{1}{2}\nabla^2\Psi-V'(\Psi)+H\right]^2 \quad (4)$$

within the set of marginal states $\Psi\in\mathcal{M}$. Here, we used Eq. (2) to express the random field in terms of Ψ. Assuming spherically symmetric instantons, the Euler-Lagrange equation takes the form

$$\left[\frac{-\Delta^{(d)}}{2}+V''(\Psi)\right]\left(\frac{\Delta^{(d)}\Psi}{2}-V'(\Psi)+H\right)\equiv\left[\frac{-\Delta^{(d+2)}}{2}+V''(\Psi)\right]\left(\frac{\Delta^{(d-2)}\Psi}{2}-V'(\Psi)+H\right)=Cn_\Psi \quad (5)$$

where $\Delta^{(d)}=\partial_r^2+\frac{d-1}{r}\partial_r$ denotes the radial part of the Laplacian in d dimensions, C is a Lagrange multiplier, and n_Ψ is the local normal to the manifold $\mathcal{M}$.

Performing an extensive search for local minima of S [analytically by solving (5) and numerically by variational minimization of (4)] we found two types of optimal random-field configurations. For $H<H_1=0.0763$, the optimal random field is such that the state Ψ corresponds to a threefold degenerate free energy minimum. However, slight deviations $\delta h(r)$ from the instanton configuration $h_{\rm inst}$ lead to a local free energy landscape where the state with lowest magnetization is marginally unstable with respect to a nearby minimum with locally higher magnetization [$\delta M\propto(\int\delta h^2)^{1/4}$]. An essentially identical analysis for $H_c<H<+\infty$, but with inverse boundary conditions $[\Psi_-\to\Psi_+]$, yields similar instantons corresponding to the dominant bubbles which implode upon increase of the external field beyond H_c [18].

A second type of instantons describes the *typical* avalanches in the interval $H_1<H<H_c$. These instantons can be found analytically by solving the "dimensionally reduced" equations of motion, $-1/2\Delta^{(d-2)}\Psi+V'(\Psi)-H=0$, which indeed yield a solutions of Eq. (5) with $C=0$. The corresponding random field is $h_{\rm inst}(r|H)=-(\partial_r\Psi)/r$. In $d=3$ dimensions, this equation is readily integrated with boundary conditions $\Psi'(r=0)=0$ and $\Psi(r\to\infty)\to\Psi_-(H)$. The action Eq. (4) associated with these field configurations decreases monotonically from $S(H_1)=5.7/\Delta$ to $S(H_{\rm sp})=0$.

An analysis of the local free energy landscape associated with this type of instantons shows that for $H_1<H<H_2=0.173$ the typical bubbles are constrained by a surface tension barrier, the change of magnetization remaining local [see Fig. 2(a)]. This is illustrated in the lower panel of Fig. 2 where we plot the instanton $h_{\rm inst}(r|H)$ together with all solutions of Eq. (2) for $H=0.13$. Initially, the system is in the marginal state (I) with the lowest magnetization. Upon slight increase of H, it becomes unstable and the system runs to the nearby lower lying minimum (II) which represents a localized bubble of positive magnetization. Further spread of this bubble is prevented by the surface tension of the domain wall that separates the positively and negatively magnetized regions. Indeed, a further saddle point (III) separates the local minimum from the global minimum (IV). Note that as long as $H<H_{dp}$, domain wall pinning by *typical* random fields will split the state (IV) into a set of metastable states which differ on larger scales which are not shown in Fig. 2.

Beyond H_2, the confining surface tension barrier vanishes, and the avalanches spread further out [cf. Figs. 2(b) and 2(c)], leading to a marked jump in the slope of the hysteresis curve. However, this effect is only observable in a small window of disorder (see Fig. 1). Indeed, for $\Delta<H_2/\alpha$, macroscopic avalanches set in before H_2, while for $\Delta\gtrsim H_2/\alpha$ the density of bubbles becomes rapidly high, preventing large avalanches as discussed below.

At a critical disorder Δ_c the typical bubbles start to percolate at the depinning field H_{dp} (see Fig. 1). This marks the crossover towards a regime with a continuous hysteresis loop. Indeed, for $\Delta>\Delta_c$ bubbles are dense already below the depinning threshold H_{dp}, such that avalanches at H_{dp} run into already positively magnetized regions and thus die out. We can estimate Δ_c from the requirement that the density of typical bubbles is $\rho(H_{dp}[\Delta_c])=\mathcal{O}(1)$, or $S(H_{dp}[\Delta_c])\simeq 1$. A more careful calculation including Gaussian prefactors yields $\Delta_c\simeq 3.2$, which translates into $\bar{\Delta}_c\simeq 9(|m^2|)^{3/2}/g\simeq\text{const}\times\tau^{3/2}/g$

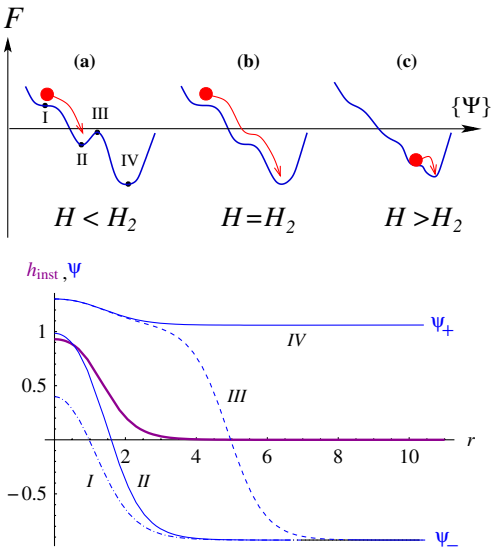

FIG. 2 (color online). Top: Schematic sketch of the free energy landscapes associated with typical avalanches for various regimes of the external field H. (a) $H<H_2$ (cf. bottom panel): The state (I) becomes unstable and runs to the metastable (II) with a local bubble of higher magnetization. It is separated from the global minimum (IV) by a surface tension barrier (III); (b) $H=H_2$: state (II) and (III) merge and the surface barrier vanishes; (c) $H>H_2$: Rare bubbles in negative random fields collapse under further increase of H. Bottom: Solutions (I-IV) of Eq. (2), obtained numerically for $H=0.13<H_2$ and $h=h_{\rm inst}(r|H)$ (thick line).

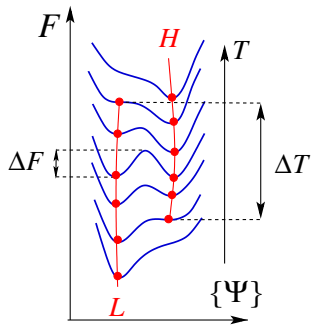

FIG. 3 (color online). Schematic view of the temperature evolution of the local free energy landscape in a random field $h_{\rm inst}(r|H=0)+\delta h$. Upon cooling, the high temperature state (H) becomes unfavorable with respect to an emerging low energy state with more uniform magnetization (L), but remains metastable in a temperature range ΔT due to a free energy barrier ΔF.

for the transition line in the $T-\Delta$ plane. It is interesting to note that for $\Delta \approx \Delta_c$ the depinning field $H_{dp}=\alpha\Delta$ is very close to the threshold field H_2 for typical avalanches to overcome surface tension barriers.

Above we used the identity of the coercive field and the depinning threshold. This applies to the infinite volume limit, as a result of which one finds $H_c[\Delta\to 0]\to 0$ (see, e.g., Ref. [19]), instead of $H_c[\Delta\to 0]\to H_{\rm sp}$, which holds for finite size systems (see bottom of Fig. 1), $H_{\rm sp}=2/3\sqrt{3}\approx 0.385$ being the spinodal field of the pure system. For a finite system of volume V, the only type of bubbles occurring in the hysteresis loop are those with sufficiently large density, $V\rho(H,\Delta)\gtrsim 1$. This relation allows us to estimate the field H^* at which the first (typical) bubbles occur. If the disorder is so weak that $H^*>H_2$, there will be a single sample spanning avalanche around the coercive field $H^*\simeq H_{\rm sp}-0.5\Delta\log[V/\xi^3]$. For stronger disorder ($H^*<H_2$) local bubbles occur at H^* while only at higher field a macroscopic avalanche is triggered by the first bubble that is not constrained by surface tension.

The analysis of instantons also provides information on the emergence and bifurcation of metastable states upon temperature variations. We have studied the temperature evolution of the free energy landscape in the presence of local random-field configurations close to the instantons corresponding to $H=0$ and $T=T_0$, $h=h_{\rm inst}(H=0;T_0)+\delta h$. These describe the rare regions which locally admit two metastable configurations in the ferromagnetic phase; cf. Fig. 3. At high temperatures there is only one state (H) in which $\Psi(r)$ adjusts to the random field. At lower temperature, a second state (L) with more uniform magnetization emerges and eventually dominates. This confirms a scenario for the emergence of metastability conjectured by Villain in the context of pinned domain walls [15]. Over a range of order $\Delta T\sim\delta^{3/2}$ [where $\delta\equiv(\int\delta h^2)^{1/2}$] the two states coexist, being separated by a free energy barrier of order $\Delta F\sim\delta^2$. The spatial density of such two-level systems with a given free energy barrier scales as $\rho(\Delta F)\propto\exp[-S_0-O(\Delta F^{1/2})]$ with $S_0=S[h_{\rm inst}(r|H=0)]\simeq 8.2/\Delta$. These two-level systems are very similar to the metastable bubbles observed numerically *above* the ferromagnetic transition [20]. We expect a deeper analysis of the bifurcation of states along the lines of this Letter to yield new insight into the nature of the phase transition in the RFIM.

We thank J. Cardy, T. Nattermann, M. Rosinberg, G. Tarjus, and, in particular, L. B. Ioffe for useful discussions. We are grateful to A. Rosso for providing us the code from Ref. [17]. This work was supported by NSF Grant No. DMR-0210575.

[1] J. P. Sethna and K. A. Dahmen, and C. R. Myers, Nature (London) **410**, 242 (2001).
[2] A. Berger *et al.*, Phys. Rev. Lett. **85**, 4176 (2000).
[3] F. Ye *et al.*, Phys. Rev. Lett. **89**, 157202 (2002).
[4] J. Marcos *et al.*, Phys. Rev. B **67**, 224406 (2003).
[5] M. C. Goh, W. I. Goldburg, and C. M. Knobler, Phys. Rev. Lett. **58**, 1008 (1987).
[6] A. Wong and M. Chan, Phys. Rev. Lett. **65**, 2567 (1990).
[7] D. Tulimieri, J. Yoon, and M. Chan, Phys. Rev. Lett. **82**, 121 (1999).
[8] J. P. Sethna *et al.*, Phys. Rev. Lett. **70**, 3347 (1993).
[9] D. Dhar, P. Shukla, and J. P. Sethna, J. Phys. A **30**, 5259 (1997).
[10] K. Dahmen and J. P. Sethna, Phys. Rev. B **53**, 14 872 (1996).
[11] O. Perkovic, K. Dahmen, and J. P. Sethna, Phys. Rev. B **59**, 6106 (1999); F. Pérez-Reche and E. Vives, Phys. Rev. B **67**, 134421 (2003).
[12] F. Detcheverry *et al.*, Phys. Rev. E **68**, 061504 (2003).
[13] See, e.g., G. Bertotti, *Hysteresis in Magnetism: For Physicists, Materials Scientists, and Engineers* (Academic Press, New York, 1998).
[14] For a lattice model with couplings J_{0i} and lattice positions r_i the criterion reads $\frac{\Delta F}{T}\sim\tau^{1/2}[(\sum_i J_{0i}r_i^2)/(\sum_i J_{0i})]^{3/2}\gg 1$.
[15] J. Villain, Phys. Rev. Lett. **52**, 1543 (1984); R. Bruinsma and G. Aeppli, Phys. Rev. Lett. **52**, 1547 (1984).
[16] H. Leschhorn *et al.*, Ann. Phys. (Leipzig) **6**, 1 (1997).
[17] Using the method of A. Rosso and W. Krauth, Phys. Rev. E **65**, 025101(R) (2002).
[18] M. Müller and A. Silva (to be published).
[19] S. Sabhapandit, D. Dhar, and P. Shukla, Phys. Rev. Lett. **88**, 197202 (2002).
[20] D. Lancaster, E. Marinari, and G. Parisi, J. Phys. A **28**, 3959 (1995).